Chapter 13

The Pathway from 5-Aminolevulinic Acid to Protochlorophyllide and Protoheme

Elena Yaronskaya
National Academy of Sciences of Belarus, Institute of Photobiology, Akademicheskaya str. 27, 22072 Minsk, Belarus

Bernhard Grimm*
Institut für Biologie/Pflanzenphysiologie, Humboldt Universität Berlin, Unter den Linden 6, D-10099 Berlin, Germany

Summary

This chapter comprehensively surveys *both* the conversion of 5-aminolevulinic acid to protochlorophyllide in the Mg-porphyrin-synthesizing branch of tetrapyrrole biosynthesis *and also* the formation of protoheme in the iron-chelating branch. This can be considered as the middle and final stages of chlorophyll and heme formation, respectively: the final conversion of protochlorophyllide to chlorophyll is discussed by Rüdiger in Chapter14 (Rüdiger). This chapter reviews the many individual enzymatic steps in these conversions, including enzyme and gene structures and the expression as well as the regulation of these steps.

*Author for correspondence, email: bernhard.grimm@rz.hu-berlin.de

Bernhard Grimm, Robert J. Porra, Wolfhart Rüdiger and Hugo Scheer (eds): Chlorophylls and Bacteriochlorophylls: Biochemistry, Biophysics, Functions and Applications, pp. 173–188.

I. Introduction

This chapter reviews the middle section of the multi-step pathway of tetrapyrrole biosynthesis whereby eight molecules of 5-aminolevulinic acid (ALA) are converted to chlorophyll (Chl) via protochlorophyllide (PChlide), or to protoheme. Eight molecules of ALA are used to generate uroporphyrinogen III (Urogen III) through a linear tetrapyrrolic intermediate, hydroxymethylbilane I (HMB). Urogen III constitutes a first branch point in tetrapyrrole biosynthesis: it can be methylated and subsequently converted to either vitamin B_{12} (cf. Battersby, 1994) or siroheme (Murphy and Siegel, 1973); alternatively it can be decarboxylated and oxidized to form protoporphyrin IX (Proto). Proto constitutes a second branch point: insertion of Fe^{2+} into Proto forms protoheme, while insertion of Mg^{2+} is the first committed step in the biosynthesis of Chl. The individual enzymatic reactions of protoheme and Chl biosynthesis, including enzyme structure, encoding gene structure and expression, as well as their metabolic regulation, are discussed.

II. Enzymes of Porphyrin Synthesis

A. 5-Aminolevulinic Acid Dehydratase (Porphobilinogen Synthase)

ALA dehydratase (porphobilinogen synthase) (ALAD) catalyzes the asymmetric condensation of two molecules of ALA to the monopyrrole, porphobilinogen (PBG) (Fig. 1) (Jordan, 1991). The bacterial, animal and plant enzymes possess structural and catalytic similarities: the exclusive Mg^{2+}-metal ion requirement, pH-optima and thiol sensitivity distinguish the plant-type ALAD from others (Senior et al., 1996). Plant ALAD contains a highly conserved metal-binding domain with Asp residues and can form active homohexameric and octameric complexes (Schaumburg and Schneider-Poetsch, 1992; Cheung et al., 1997). ALAD from other eukaryotic and prokaryotic organisms is octameric, requires both Mg^{2+} and Zn^{2+} and coordinates the latter through Cys and His in the metal-binding domain. X-ray structures of yeast and bacterial ALAD have been presented (Erskine et al., 1999; Frankenberg et al., 1999). Recent structural analysis shows that human allelic ALAD differs from the wild-type protein by an ability to shift between the octameric and hexameric form: this transition appears relevant in a Mg^{2+}-dependent allosteric regulation of ALAD, as only the octameric form makes a Mg^{2+} binding site available (Breinig et al., 2003).

The soluble plant ALAD was located in plastids from pea leaves or arum lily spadices (Smith, 1988). The plant *ALAD* gene encodes a precursor for plastid translocation. Light differently affects *ALAD* gene expression in various plant species. *ALAD* mRNA levels are unchanged during greening of pea leaves, while the enzyme activity increases: a post-transcriptional light-dependent control of this enzymatic step has been proposed (Boese et al., 1991). In soybean, *ALAD* mRNA accumulates during greening without an apparent change in enzyme activity or protein level (Kaczor et al., 1994). An increase in both *ALAD* mRNA and enzyme activity during light exposure corresponds in light-dark synchronized cells of *Chlamydomonas (C.) reinhardtii* with the rate of Chl accumulation (Matters and Beale, 1995a). Although *ALAD* mRNA accumulates under blue light, the *ALAD* gene is also controlled through the cell cycle or the circadian clock (Matters and Beale, 1995b).

B. Porphobilinogen Deaminase (Hydroxymethylbilane Synthase)

Porphobilinogen deaminase (PBGD) catalyzes the condensation of four molecules of PBG into the linear hydoxymethylbilane I (HMB) which is unstable and spontaneously cyclizes to Urogen I (Battersby et al., 1979a) when the succeeding enzyme, uroporphyrinogen III synthase (UROS) is absent, defective or limiting: for example, Uro I, the oxidation product of Urogen I, has been isolated from the urine of the

Abbreviations: ALA – 5-aminolevulinic acid; ALAD – 5-aminolevulinic acid dehydratase; BChl – bacteriochlorophyll; *C.* – *Chlamydomonas*; Chl – chlorophyll; *Chl.* – *Chlorobium*; Chlide – chlorophyllide; Copro – coproporphyrin; Coprogen – coproporphyrinogen; CPO – coproporphyrinogen oxidase; CsCl – cesium chloride; HMB – hydroxymethylbilane I; Mg-chelatase – magnesium protoporphyrin IX chelatase; MgProto – magnesium protoporphyrin IX; MgProtoMe – magnesium protoporphyrin IX monomethylester; MgProtoMeC – magnesium protoporphyrin IX monomethylester cyclase ; MTF – magnesium protoporphyrin IX monomethyl transferase; PBG – porphobilinogen; PBGD – porphobilinogen deaminase; PChlide – protochlorophyllide; POR – protochlorophyllide oxidoreductase; PPOX – protoporphyrinogen oxidase; Proto – protoporphyrin IX; Protogen – protoporphyrinogen IX; *Rba.* – *Rhodobacter*; *Rvi.* – *Rubrivivax*; *Rvu.* – *Rhodovulum*; ROS – reactive oxygen species; Uro – uroporphyrin; UROD – uroporphyrinogen III decarboxylase; Urogen – uroporphyrinogen; UROS – uroporphyrinogen III synthase

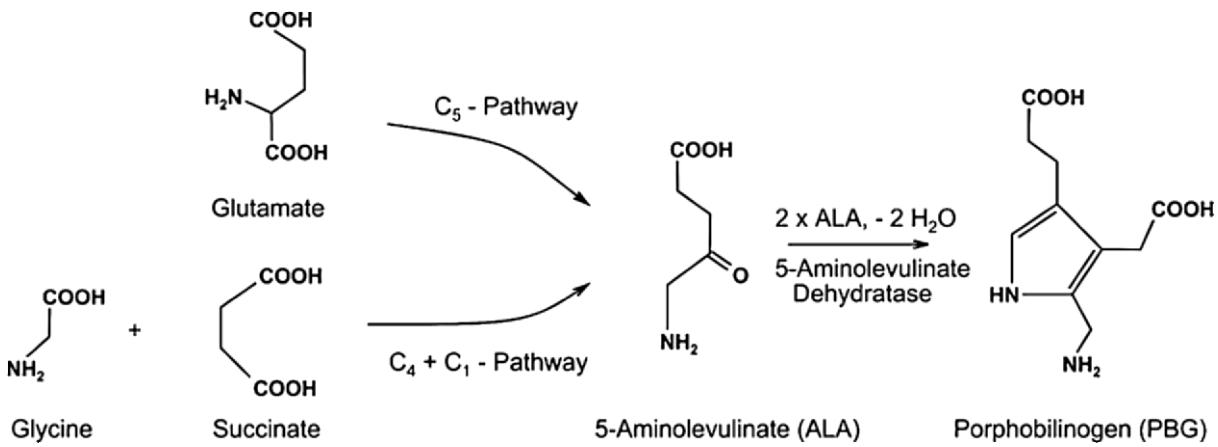

Fig. 1. Two pathways for biosynthesis of ALA, the committed molecule of tetrapyrrole biosynthsis and the subsequent asymmetric condensation of two molecules ALA to porphobilinogen.

congenital porphyria patients (Rimington and Miles, 1951) and coproporphyrin (Copro) I, the oxidation product of coproporphyrinogen (Coprogen) I, which is formed by enzymatic decarboxylation of Urogen I (see Section II.D), has been isolated from anoxic yeast cells (Porra et al., 1973). Coprogen I is not a substrate for Coprogen III oxidase (Section II.E). In the presence of UROS, however, HMB is directly converted to Urogen III (Battersby et al., 1979b; Jordan and Seehra, 1979), an intermediate common to the biosynthesis of protoheme and Chl. The synthesis of HMB involves, as a preparatory step, the synthesis of a unique enzyme-bound dipyrromethane cofactor, which serves as an attachment point for the subsequent assembly of four PBG molecules to form a hexapyrrole (Fig. 2) (Hart et al., 1987; Jordan and Warren, 1987). In *E. coli,* the newly synthesized dipyrromethane cofactor is post-translationally attached to Cys242 of the apoprotein by a thioether linkage. Sequential condensation of four PBG molecules commences at the free α-position of the cofactor. Once the hexapyrrole stage is reached, a linear tetrapyrrole, HMB, is released before the enzyme-dipyrrole complex accepts more PBG molecules (Battersby et al., 1983). X-ray structural studies of the *E. coli* enzyme suggest the stepwise elongation of the polypyrrole chain (Louie et al., 1996). Examination of wild type and mutants revealed essential amino acids for cofactor binding and for enzyme-intermediate complex formation during chain elongation at the catalytic side (Louie et al., 1996). The same amino acids are also conserved in plant and algal PBGD which occurs in the plastid stroma. The pea and *Arabidopsis* precursor proteins have an approximate Mr of 40 kDa: after import into isolated chloroplasts, the Mr of the mature protein was 35 kDa (Witty et al., 1993; Lim et al., 1994). Expression of the pea gene is strongly induced by light: steady-state levels of *PBGD* mRNA increase in parallel with enzyme activity (Witty et al., 1993).

C. Uroporphyrinogen III Synthase (UROS)

UROS simultaneously catalyzes the cyclization and isomerization of HMB by the inversion of ring D to yield the first isomer III cyclic tetrapyrrole, Urogen III, which is the first common tetrapyrrolic intermediate of heme and Chl. Inversion of ring D probably involves formation of a *spiro*-cyclic-intermediate (Fig. 2) (Crockett et al., 1991; Stark et al., 1993). The instability of HMB apparently requires a PBGD-UROS complex in vivo, since an alteration of the sedimentation rate of wheat germ PBGD (Higuchi and Bogorad, 1975) and of the k_m for PBG of the *Euglena* enzyme occurs in the presence of UROS (Battersby et al., 1979a). Purified UROS from *Euglena* is a monomer (Mr = 31 kDa) (Hart and Battersby, 1985). Structural determination by X-ray crystallography of the human enzyme revealed a bilobed structure of a homodimer. Mutation of various residues in the putative active site cleft revealed no essential residue for the catalytic mechanism (Mathews et al., 2001; Schubert et al., 2002).

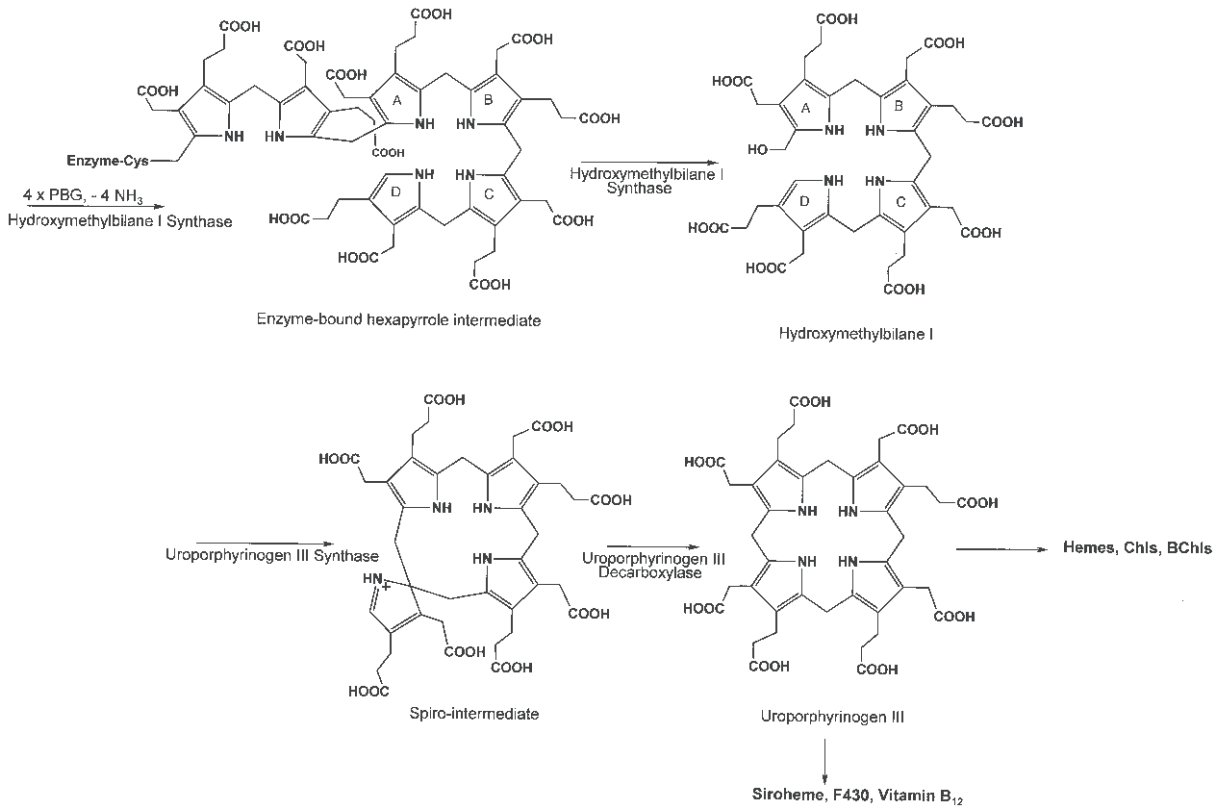

Fig. 2. Enzymatic steps of the tetrapyrrole biosynthetic pathway from porphobilinogen to uroporphyrinogen III.

D. Uroporphyrinogen III Decarboxylase

Uroporphyrinogen III decarboxylase (UROD) is located at the first branch point of the tetrapyrrole biosynthetic pathway: decarboxylation of Urogen III leads to the biosynthesis of protoheme and of Chl or bacteriochlorophyll, whereas its C-methylation initiates synthesis of vitamin B_{12} (Battersby, 1994) and sirohemes (Murphy and Siegel, 1973). UROD catalyzes the decarboxylation of all four acetate side-chains of Urogen III resulting in Coprogen III formation (Fig. 3). Decarboxylation starts from pyrrole ring D followed by a clockwise decarboxylation at rings A, B, and C (Luo and Lim, 1993). Urogen I can also serve as substrate for UROD but the product, Coprogen I, cannot be further metabolized.

All homologous plant UROD sequences, which are derived from cDNA sequences, possess an N-terminal extension for plastid translocation. The recombinant tobacco UROD forms a homodimeric structure under similar ionic strength conditions found in the plastidic stroma fraction. X-ray crystal structure of tobacco UROD (Martins et al., 2001) confirmed the previously published 3D-structure of the homologous human enzyme (Whitby et al., 1998). The analysis reveals one catalytic cleft per monomer with six invariant polar residues. Asp82/86 and Tyr159/164 (tobacco/human enzyme numbering) seem to be the catalytic functional residues, which may serve in substrate recognition and binding. Arg32/37 is proposed to direct the substrate into the hydrophobic catalytic cleft (Whitby et al., 1998; Martins et al., 2001).

URODD mRNA and protein levels increased during greening of etiolated barley leaves (Mock et al., 1995). The expression of *URODD* antisense RNA in tobacco plants leads to the formation of necrotic leaf lesions, which are caused by generating reactive oxygen species (ROS) as a result of accumulating photo-reactive Uro III. The transgenic plants analyzed possessed a minimal wildtype activity of 70% (Mock and Grimm, 1997). The photo-destructive processes in leaves induced an anti-oxidative defense system in several cellular compartments and diminished the total content of reduced low-molecular-mass

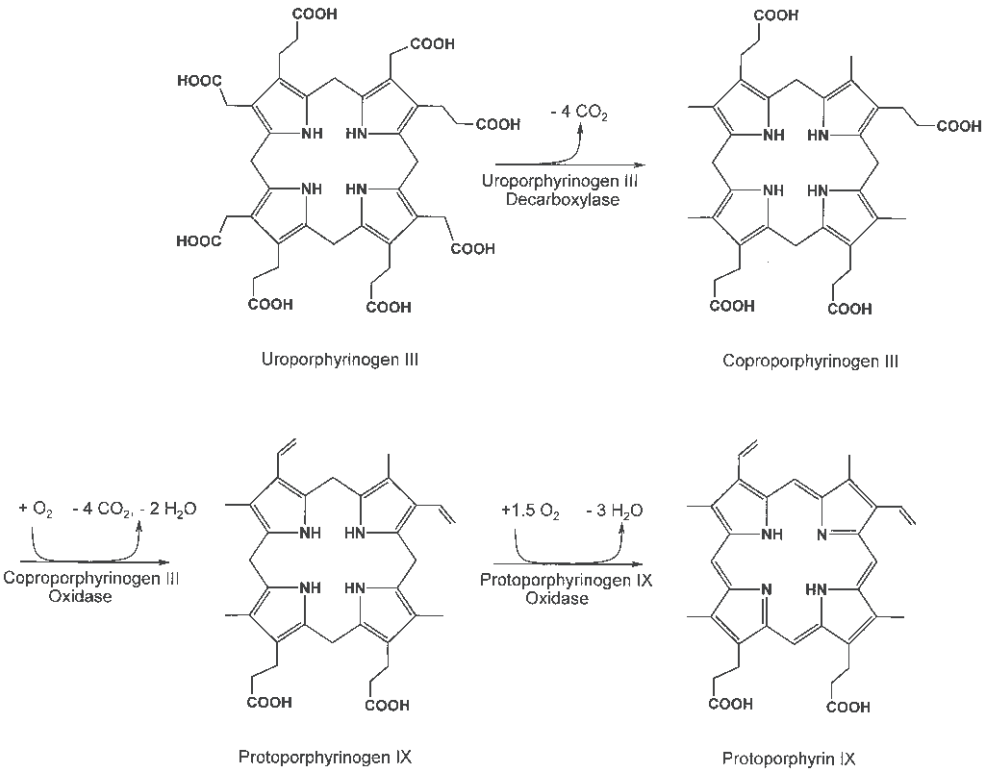

Fig. 3. Enzymatic steps of the tetrapyrrole biosynthetic pathway from uroporphyrinogen III to protoporphyrin IX.

anti-oxidants (Mock et al., 1998). The maize *Les22* mutant carries a mutant *UROD* gene and also shows necrotic lesions (Hu et al., 1998). A similar effect of Uro(gen) III accumulation was observed after cesium chloride (CsCl) treatment of greening barley leaves. However, the excess Urogen III was re-metabolized when the toxic metal cations were removed after less than 8 h of CsCl incubation. Upon longer CsCl exposure, accumulated Uro generated necrotic lesions. It is assumed that photodynamic damage of leaves begins when photoprotective activities were overwhelmed with Urogen, which was infiltrated into the cytoplasm (Shalygo et al., 1997, 1998).

E. Coproporphyrinogen III Oxidase

Coprogen III oxidase (CPO) catalyzes the oxidative decarboxylation of the two propionate side chains of ring A and B to vinyl groups to yield the divinyl compound, protoporphyrinogen IX (Protogen) (Fig. 3). Coprogen I cannot serve as substrate for this enzyme. Analysis of CPO activity in different subcellular compartments of pea and spadices of cuckoo-pint, as well as immuno-detection of CPO in soybean, revealed the exclusive location of this enzyme in plastids (Smith et al., 1993). *CPO* gene expression showed tissue-specific and developmental changes rather than changes upon light exposure or under diurnal and circadian growth conditions (Kruse et al., 1995a; Papenbrock et al., 1999). The content of mRNA reached its maximum in young developing cells and drastically decreased in older differentiated cells. Roots from soybean and pea synthesized elevated levels of CPO during nodulation and displayed also higher activities of ALAD, PBGD, protogen oxidase (PPOX) and ferrochelatase indicating the plant's contribution to plant protoheme biosynthesis for the assembly of cytochrome as well as of nodule leghemoglobin (Santana et al., 1998).

Reduction of CPO activity by antisense RNA expression led, in transgenic tobacco plants, to an accumulation of Copro(gen) and consequently to light-intensity-dependent leaf necrosis (Kruse et al., 1995b). Although the protective system against ROS was generally alerted, the ascorbate and glutathione concentrations were decreased relative to control plants, suggesting that anti-photosensitization processes could not be sufficiently invoked to prevent cell

death (Kruse et al., 1995b; Mock et al., 1998). Likewise, in *UROD* antisense transgenic lines, CPO-deficient plants induced several defense responsive genes resembling the hypersensitive reaction observed in response to pathogen attack (Mock et al., 1999). The recessive *Arabidopsis* lesion initiation (*lin2*) mutant contains a defective gene encoding CPO and forms development- and light-dependent necrotic lesions in leaves and siliques (Ishikawa et al., 2001)

F. Protoporphyrinogen IX Oxidase

Protogen oxidase (PPOX) is the last enzyme common to both Chl and protoheme biosynthesis. This flavin-requiring enzyme catalyzes the six-electron oxidation of Protogen to Proto (Fig. 3) and its activity was detected in plants in both plastids and mitochondria (Jacobs and Jacobs, 1987; Smith et al., 1993). Two different genes, PPOX I and PPOX II, exist in different plant species (e.g., Lermontova et al., 1997; Che et al., 2000; Watanabe et al., 2001). Identical isoforms from different plant species show a high degree of identity (e.g., PPOX II isoforms share approximately 70% identical amino acids), while the sequence identity between isoform I and II of the same species is relatively low (28%). PPOX is the first enzyme of the tetrapyrrole biosynthetic pathway to be located in two different subcellular compartments: the mitochondrion and the chloroplast. The spinach PPOX I enzyme is preferentially associated with the stromal side of the thylakoid membrane, but a small portion is also found on the stromal side of the inner envelope membrane (Che et al., 2000). The spinach *PPOXII* gene encodes two translation products of different size, 59 kDa (PPOX IIL) and 55 kDa (PPOX IIS), by use of two in-frame initiation codons. In situ immunological analysis, by electron microscopy with anti-PPOX II, confirmed the translocation of a 57 kDa PPOX IIL in the inner plastid envelope fraction facing the stromal side while the 55 kDa PPOX IIS was located in the inner mitochondrial membrane fraction (Watanabe et al., 2001).

PPOX is the target enzyme of phthalimide- and diphenylether-type herbicides (Scalla et al., 1990; Duke et al., 1991). The inhibition of PPOX by these photodynamically-acting herbicides causes accumulation of Protogen, which leaks out of plastids and is oxidized to Proto by unspecific herbicide-resistant peroxidases bound to plasma membranes (e.g., Jacobs and Jacobs, 1993). Excessive Proto concentrations are known to cause a potent phytotoxic photosensitization, which results in the generation of lethal amounts of ROS causing membrane peroxidation and cell death (Matringe and Scalla, 1988).

Genetic and biochemical analyses were performed to characterize herbicide-resistant mutants. A single nucleotide substitution (G → A) in the *PPOX* gene of *C. reinhardtii* caused an amino acid alteration (Val291Met) which conferred herbicide tolerance (Randolph-Anderson et al., 1998). An *Arabidopsis* mutant with two substitutions in PPOX I (Tyr426Met and Ser305Leu) was 600-fold more tolerant to PPOX inhibitors (Li et al., 2003). Herbicide tolerance of the photomixotrophic tobacco YZI-1S cell line was explained by amplification of the *PPOX II*-gene leading to increased levels of the corresponding mRNA and a five-fold increase of the mitochondrial enzyme activity (Watanabe et al., 1998, 2002). Transgenic tobacco or rice plants became more resistant to oxyfluorfen by expressing a *B. subtilis PPOX* gene (Choi et al., 1998; Lee et al., 2000). Over-expression of *Arabidopsis PPOX I* gene made transgenic tobacco more resistant to acifluorfen (Lermontova and Grimm, 2000).

The genetic or chemical disruption of the metabolic pathway at the step of Proto synthesis can also induce several defense responses as a result of porphyrin-induced photosensitization. *Arabidopsis* plants expressing *PPOX* antisense genes display the known pattern of necrotic leaf lesions resembling lesions after pathogen-induced hypersensitivity reactions (Molina et al., 1999). Different inhibitors were applied to clarify structural properties of the active site of PPOX (Arnould and Camadro, 1998; Arnould et al., 1998; Birchfield et al., 1998). The crystal structure of a PPOX has recently been published (Koch et al., 2004).

III. The Chlorophyll-synthesizing Branch

A. Mg-Protoporphyrin IX Chelatase

Magnesium protoporphyrin IX chelatase (Mg-chelatase) catalyzes the insertion of Mg^{2+} into Proto and, thus, directs Proto into the Chl biosynthesizing branch (Fig. 4). The complexity of the structural, enzymatic and regulatory properties of Mg-chelatase has been addressed in numerous studies. The protein consists of three different subunits. Transposon mutagenesis studies in *Rba. capsulatus* (Bollivar et al., 1994b) and *Rba. sphaeroides* (Gorchein et al., 1993) have initially demonstrated that the expression of the three gene products *BchI, -D* and *-H,* are required for Mg-chelatase activity. The homologous proteins in plants,

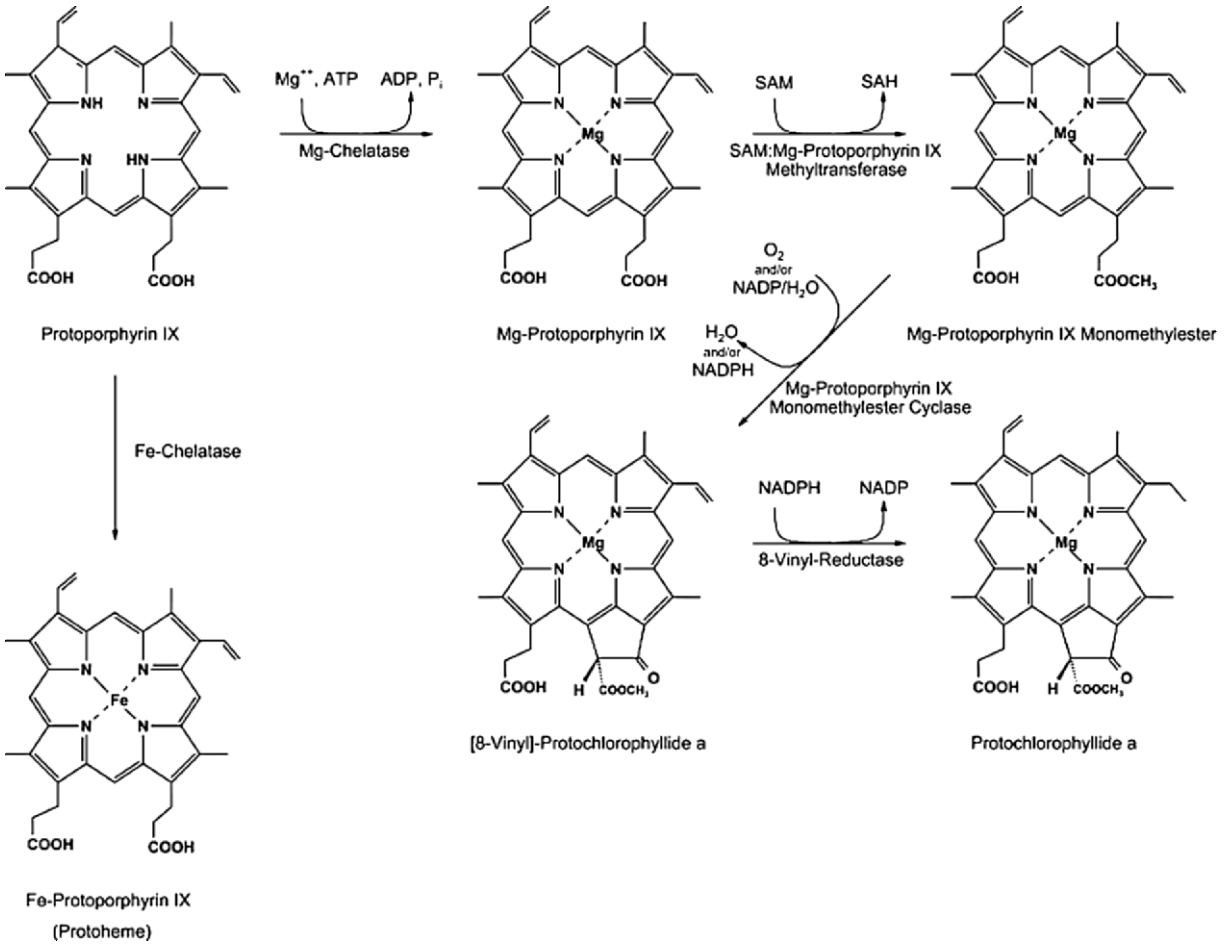

Fig. 4. Enzymatic steps of the tetrapyrrole biosynthetic pathway at the branchpoint to chlorophyll and protoheme biosynthesis. Protoporphyrin IX is either directed into the Mg branch and subsequently converted into protochlorophyllide or into the Fe branch to form protoheme.

algae and cyanobacteria are named CHLI/XAN-H, CHLD/XAN-G, and CHLH/ XAN-F with molecular masses 36–46 kDa, 60–87 kDa and 123-150 kDa, respectively (LCD Gibson et al., 1995, 1996; Jensen et al., 1996a,b; Papenbrock et al., 1997; Petersen et al., 1998). The *ChlI* homologous gene is encoded in the chloroplast genome of most algae and *Euglena gracilis* (Orsat et al., 1992).

By analysis of *Arabidopsis thaliana* (*cs*) and *Antirrhinum majus* (*olive*) mutants, the first plant genes encoding two different subunits of Mg-chelatase were detected (Koncz et al., 1990; Hudson et al., 1993). In barley, the *Xantha-f, Xantha-g* and *Xantha-h* loci were assigned to the structural genes for the three different subunits of Mg-chelatase (Jensen et al., 1996b; Petersen et al., 1999).

Mg-chelatase activities were detected in intact cucumber chloroplasts (Castelfranco et al., 1979), in broken pea chloroplasts (Walker and Weinstein, 1991), in a sub-plastid membrane fraction without a soluble stroma fraction (Lee et al., 1992) and, subsequently, in totally soluble fractions of pea chloroplasts (Guo et al., 1998). Enzyme assays with recombinant *Rba. sphaeroides, Synechocystis* PCC 6803 and *Chlorobium* (*Chl.*) *vibrioforme* subunits revealed that all three proteins were required to reconstitute the Mg-chelatase activity in vitro (LCD Gibson et al., 1995; Jensen et al., 1996a; Willows et al., 1996; Petersen et al., 1998; Willows and Beale, 1998). A stoichiometry of 4 BchI:1 BchD and 2 CHLI:1 CHLD:4 CHLH was found to be optimum in in vitro reconstitution assays with the three recombinant subunits from *Rhodobacter* and *Synechocystis*, respectively (Willows et al., 1996; Hansson et al., 1999; Jensen et al. 1999a).

Analysis of the 3-D structure of the *Rba. capsulatus*

BchI protein revealed that the I-subunit belongs to a chaperone-like family of AAA^+ proteins (possessing ATPase properties associated with various cellular activities) and is proposed to form a hexameric ring structure with a ring diameter of about 110 Å (Fodje et al., 2001). The N-terminal domain of BchI contains Walker A and Walker B motifs, which are generally present in nucleotide triphosphate-hydrolyzing enzymes (Hansson et al., 2002). Due to the structural similarity to BchI, the N-terminus of BchD possibly contains an AAA module and, additionally, an integrin I domain at the C-terminus (Fodje et al., 2001). An integrin I-domain-binding motif was proposed in the C-helical domain of BchI and BchH which could allow interaction of all subunits through BchD and, thus, establishing a linkage between porphyrin metalation by BchH and ATP hydrolysis by BchI (Fodje et al., 2001).

The initial enzymatic studies by several groups permitted an advanced model for the molecular organization and the mechanistic steps of Mg-chelatase. This model proposed that, firstly, an ATP-dependent double-ring structure consisting of BchI and BchD is formed, which hinders the ATPase activity of BchI (Walker and Willows, 1997; Fodje et al., 2001). Secondly, a ternary complex with the substrate-binding BchH is formed upon addition of Mg^{2+} which instigates porphyrin metalation. Then, release of the BchI-ATP-binding site occurs by weakening the protein-protein interaction at the integrin I-domain which triggers ATP hydrolysis (Fodje et al., 2001). These enzymatic analyses of bacterial Mg-chelatase resemble those of recombinant subunits from *Synechocystis* and recombinant tobacco subunits expressed in yeast (Grafe et al., 1999).

Expression of both the *Xan-f/CHLH* and *Xan-h/CHLI* gene in etiolated barley seedlings, in young tobacco plants and in photomixotrophic soybean suspension cultures is light-induced, but *CHLH mRNA* always accumulated more rapidly upon illumination than *CHLI mRNA* (Jensen et al., 1996b; Kruse et al., 1997; Nakayama et al., 1998). The barley Mg-chelatase activity increased three- to four-fold during greening, reaching a maximum after 6 h in light (Petersen et al., 1999). Thus, it is generally accepted that the capacity of Mg-chelatase activity correlates with the expression profile of *XAN-F/CHLH* (Jensen et al., 1996b; Papenbrock et al., 1997; Petersen et al., 1999).

In barley, *Arabidopsis,* tobacco and soybean, the *XAN-F/CHLH* expression was under the control of the circadian clock with a maximum at the beginning of the light period and a minimum at the transition from light to dark (Jensen et al., 1996b; Nakayama et al., 1998; Papenbrock et al., 1999). In contrast, the *CHLI* transcripts remained constant (LCD Gibson et al., 1996; Papenbrock et al., 1999). The tobacco *CHLD m*RNA content inversely oscillated to the *CHLH* level in tobacco over a 24-h light-dark cycle (Papenbrock et al., 1999).

Mg-chelatase subunits can exhibit Mg^{2+}-dependent changes in their distribution between stroma and chloroplast membranes (LCD Gibson et al., 1996; Nakayama et al., 1998; Luo et al., 1999). CHLH is largely soluble at low Mg^{2+} concentrations but attaches to the envelope membrane at Mg^{2+} concentration above 5 mM. The association of CHLD with envelope membranes shows a similar Mg^{2+} dependency. However, while CHLI was detected in the soluble fraction, regardless of the Mg^{2+} concentration, the importance of the sub-compartmental (stroma/membrane) distribution of Mg-chelatase for modulation of its activity remains an open question.

Mutants, lacking one of the subunits, and transgenic plants, with deregulated expression of one of the subunits, illustrate interesting effects on Chl biosynthesis and chloroplast development. Barley *Xantha-h* mutants lack *not only* the XAN-H (CHLI) *but also* the XAN-G (CHLD) subunit (Hansson et al., 1999; Petersen et al., 1999). In contrast, in *Arabidopsis* T-DNA knockout mutants of the *CHLI* locus show wild type *CHLD* mRNA content (Rissler et al., 2002). It was proposed that the *CHLI2* gene product is responsible for a limited CHLD accumulation and, consequently, for Mg-chelatase activity and Chl accumulation in this mutant. Silencing of the tobacco *CHLH* gene by infection with tobacco mosaic virus vectors containing *CHLH* inserts resulted *not only* in strongly decreased levels of *CHLH* mRNA, *but also* of *CHLD* mRNA (Hiriart et al., 2002).

Transgenic tobacco plants expressing antisense *CHLI* and *CHLH* mRNA, respectively, displayed a chlorotic phenotype and reduced plant-growth rate. The loss of Chl correlated with the gradually reduced Mg-chelatase activity in response to antisense inactivation (Papenbrock et al., 2000a,b). In spite of diminished Mg-chelatase activity, the metabolic substrate, Proto, did not accumulate. Lower heme contents exclude the possibility of re-direction of non-metabolized Proto into heme biosynthesis in the transgenic plants. ALA synthesizing capacity was diminished in parallel with reduced Mg-chelatase activ-

ity and was due to lower levels of transcripts encoding glutamyl-tRNA reductase and ALAD (Papenbrock et al. 2000a, Chapter 16, Beck and Grimm).

The barley *chlorina-125, -157,* and *-161* mutants contain point mutations in the *CHLI* gene and display a semi-dominant phenotype due to simultaneous expression of mutant and wild type CHLI. A small proportion of wild-type hexamers rescues the heterozygous plants but cannot provide sufficient Mg-chelatase activity to produce wild-type levels of Chl (Hansson et al., 1999, 2002). Both the *Arabidopsis cs* mutant (Koncz et al., 1990) and the virus-induced silencing of the *sulfur* allele in *Nicotiana benthamiana* (Kjemtrup et al., 1998) display chlorotic phenotypes similar to the *CHLI* antisense plants.

Four out of five *Arabidopsis gun* mutants (genome unregulated) are affected in the expression of genes involved in tetrapyrrole biosynthesis. *Gun5* encodes the CHLH subunit of Mg-chelatase and revealed a point mutation in the *CHLH* gene (Mochizuki et al., 2001; for more details see chapter 16, Beck and Grimm). The allelic Chl-less *C. reinhardtii* mutants, *chl-1* and *brs-1,* could only grow heterotrophically in the dark because of Proto-mediated extreme light sensitivity. The genetic lesions could be assigned to frameshift mutations in the *CHLH* gene, respectively, resulting in a CHLH deficiency, but without alteration in expression of *CHLI* and *CHLD* genes (Chekounova et al., 2001; Chapter 16, Beck and Grimm).

B. S-Adenosyl-L-Methionine:Mg-Protoporphyrin IX Methyltransferase (MTF)

This MTF enzyme catalyzes the transfer of a methyl group from S-adenosyl-methionine to the carboxyl group of the 13-propionate side-chain of MgProto to yield MgProto monomethylester (MgProtoMe) (Fig. 4) (KD Gibson et al., 1963; Ellsworth and Dullaghan, 1972). A ping-pong type mechanism was demonstrated for the plant MTF enzyme (Ellsworth et al., 1974). Expression of the recombinant *BchM/ChlM* from *Rba. sphaeroides, Rba. capsulatus* and *Synechocystis* PCC 6803 revealed a monomeric enzyme of 25–27 kDa (Bollivar et al., 1994a; LCD Gibson and Hunter, 1994; Smith et al., 1996). Consistent with previous suggestions about a Mg-chelatase-MTF complex (Gorchein, 1972), addition of soluble BchH from *Rba. capsulatus* increased seven-fold the activity of recombinant MTF (Hinchigeri et al., 1997), and soluble extracts of cell cultures co-expressing *BchM* and the three Mg-chelatase subunits readily converted Proto to MgProtoMe (Jensen et al., 1999b).

The first plant cDNA sequences encoding MTF with an N-terminal plastid transit sequence were described for *Arabidopsis thaliana* and *Nicotiana tabacum* (Block et al., 2002; Alawady and Grim, 2005; Alawady et al., 2005). It is suggested that a hydrophobic region in the N-terminal half of the mature protein is responsible for anchoring the protein to both the envelope and thylakoid membranes (Block et al., 2002).

C. Mg-Protoporphyrin IX Monomethylester Cyclase (MgProtoMeC)

This oxidative cyclase enzyme catalyzes the complex reaction sequence for formation of the isocyclic ring, which is derived from the C-13-methylpropionate side chain of MgProtoMe (Fig. 4). The reaction sequence consists of three steps: hydroxylation of the methylpropionate side chain at the C-13^1 carbon atom, oxidation of this C-13^1-hydroxyl to a C13^1-oxo group and ligation of the C-13^2 carbon of the newly-formed 13^1-oxo-methylpropionate side chain to the C-15 bridge carbon between pyrrole rings C and D (Wong et al., 1985; Bollivar and Beale, 1996). The oxidative formation of the oxo group is facilitated by methylation of the carboxylate group to prevent its decarboxylation. Two mechanisms of cyclization were found in the tetrapyrrole pathway. In higher plants and green algae, the oxo-group oxygen is derived from molecular oxygen (Chereskin et al., 1982) by an oxygenase mechanism, while a different hydratase-type enzyme in *Rba. sphaeroides* uses oxygen from water under anaerobic conditions (Porra et al., 1995). *Rhodovulum (Rvu.) sulfidophilum,* which forms BChl *a* aerobically in the dark or anaerobically in the light, possesses both the oxygenase and hydratase pathways which can operate simultaneously in aerobic conditions (Porra et al., 1998). Anaerobic isocyclic ring formation for bacteriochlorophyll synthesis in *Rba. capsulatus* was shown to require a cobalamine cofactor (Gough et al., 2000).

Cyclase activity in developing cucumber chloroplasts, wheat etioplasts and *Synechocystis* require a membrane-bound and soluble fraction (Wong and Castelfranco, 1984; Nasrulhaq-Boyce et al., 1987; Walker et al., 1991), while the activity of *C. reinhardtii* was exclusively associated with membranes of lysed chloroplasts (Bollivar and Beale, 1995, 1996). Addition of iron chelators, but not of CO, KCN and NaN_3, inhibited cyclase activity suggesting that nonheme

iron is involved in the reaction (Nasrulhaq-Boyce et al., 1987; Whyte et al., 1992; Bollivar and Beale, 1995, 1996).

Disruption of the *orf358(ascF)* gene in the purple bacterium *Rubrivivax (Rvi.) gelantinosus,* which can form BChl *a* under aerobic growth conditions, causes accumulation of MgProtoMe aerobically indicating that the encoded protein is involved in the subsequent oxidative cyclization step (Pinta et al., 2002). Sequence comparison revealed homology with both the *Crdl* gene of *C. reinhardtii,* which was initially identified by a mutant screen for copper deficiency (Moseley et al., 2002), and also with the *PNZIP* gene in *Pharbitis nil*, which was characterized by phytochrome and endogenous clock induction (Zheng et al., 1998). The encoded protein belongs to the family of di-iron carboxylate proteins, characterized by an iron binding motif consisting of six conserved amino acids (four carboxylate residues and two histidines) (Berthold and Stenmark, 2003). In *Rba. capsulatus,* the *BchE* gene was identified as essential for anaerobic isocyclic ring formation (Bollivar et al., 1994a, b).

It is still not clear whether these homologous proteins (AscF/Crd1/PNZIP) can perform the whole reaction or whether other protein components are required for the entire reconstitution of the enzyme activity. The requirement of at least two plastidal protein fractions for the cyclization reaction was predicted after biochemical analysis of cyclase activity of two different barley mutants, *Xantha l-35* and *viridis K-23* (Walker and Willows, 1997). Thus, it is assumed that the *acsF* gene of *Rvi. gelatinosus* encodes at least a MgProtoMe hydroxylase (Pinta et al., 2002; Berthold and Stenmark, 2003)

D. Vinyl Reductase

8-Vinyl reductase catalyzes the conversion of an 8-vinyl group on ring B to an ethyl group (Fig. 4). Enzyme activity was measured in isolated plastid membranes from cucumber cotyledons, maize and barley (Parham and Rebeiz, 1992). This reaction can be carried out at least at two different steps in the pathway transforming divinyl-PChlide into monovinyl-PChlide or divinyl-Chlide into monovinyl-Chlide (Rebeiz et al., 1983; Tripathy and Rebeiz, 1988). Monovinyl-PChlide and -Chl are mainly found in plants. In the necrotic maize mutant (ON 8147), photosynthetic pigments are represented almost exclusively by divinyl Chl *a* and *b* but, in darkness, divinyl-PChlide is the main Chl precursor. Disruption of the *Rba. capsulatus bchJ* gene leads to increased divinyl-PChlide and lowered bacteriochlorophyll concentrations. Thus, *bchJ* was thought to be a candidate for the structural gene of this enzyme (Bollivar et al., 1994b; Suzuki and Bauer, 1995). But very recently, the first plant gene encoding 8-vinyl reductase was identified by map-based cloning of an *Arabidopsis* mutant that accumulated divinyl-Chl (Nagata et al., 2005). This gene has no similarity to *bchJ* of *Rhodobacter*. Divinyl-Chls *a* and *b* are major pigments in some type II cyanobacteria (Goericke and Repeta, 1993).

IV. The Protoheme-synthesizing Branch

A. Ferrochelatase

The enzyme ferrochelatase (protoheme ferrolyase) is a single membrane-associated- and ATP-independent-protein requiring only Fe^{2+} and Proto as substrates for the final step of heme formation. Ferrochelatase is considered to play an important role in the regulation of metabolite distribution at the branch point of porphyrin biosynthesis. Ferrochelatase activity has been demonstrated in both plant plastids and mitochondria (Porra and Lascelles, 1968). More recently, plastid ferrochelatase was associated *either* with thylakoid membranes in peas (Matringe et al., 1994) *or* with thylakoid and envelope membrane in *Arabidopsis* (Roper and Smith, 1997; Masuda et al., 2003).

The crystal structure of *Bacillus subtilis* and human ferrochelatases indicates that while the major features of the chelation reaction are conserved (Lecerof et al., 2000; Wu et al., 2001) differences were revealed in molecular size, subunit composition, solubility and presence or absence of a [2Fe-2S]-cluster between bacterial, plant and human ferrochelatases (Dailey et al., 2000). Mechanisms of porphyrin distortion and metalation were proposed for the bacterial enzyme, under the assumption that the enzyme attaches to pyrrole rings B, C and D and forces a tilt in ring A, which allows the metal to enter the porphyrin via the distorted pyrrole (Lecerof et al., 2000).

cDNA sequences encoding plant ferrochelatase were obtained from cucumber, barley (*HEMH*; Miyamoto et al. 1994) and *Arabidopsis* (*AtFC-I,* Smith et al., 1994) by complementation of the bacterial or yeast ferrochelatase mutants. Subsequently, a second *Arabidopsis* cDNA sequence (*AtFC-II*) was found that encodes another precursor ferrochelatase

with a 69% identity to AtFCI (Chow et al., 1998). AtFC-I was expressed in all plant tissues and could be imported in vitro both into pea chloroplasts and mitochondria, whereas *AtFC-II* was expressed only in leaves, stems and flowers, where it was solely targeted to chloroplasts (Chow et al., 1998; Singh et al., 2002): *ATFC-II* was not expressed in roots. The importation properties of AtFC1, reported above to be dual-targeted into mitochondria and plastids, have recently been re-evaluated. Both AtFC1 and AtFC2 could not be imported into *Arabidopsis* mitochondria, suggesting that the presence of ferrochelatase in plant mitochondria should be re-investigated (Lister et al., 2001). However, calculations about the contribution of mitochondrial ferrochelatase to the total activity in roots, green and etiolated leaves revealed 30% of total activity in tobacco mitochondria (Papenbrock et al., 2001) and less than 10% in pea mitochondria (Cornah et al., 2002). Only traces of activity, however, were found in cucumber mitochondria (Masuda et al., 2003); indeed, both ferrochelatase isoforms were immunologically detected in plastids but not in mitochondria (Masuda et al., 2003).

Supporting the studies of Chow et al (1998), but not of Lister et al. (2001), the cucumber *CsFeC1* gene, which is homologous with *AtFC1*, showed a light-insensitive expression in non-photosynthetic tissues, such as hypocotyls and roots, but not in cotyledons (Suzuki et al., 2002) and could be imported into mitochondria. The *CsFeC2* mRNA was detected in all tissues and strongly light-induced in cotyledons (Suzuki et al., 2000, 2002). The protein was predominantly translocated to thylakoid membranes and, to a lesser extent, to the envelope membranes. It has been suggested that two routes operate concurrently in plastids for ALA biosynthesis and its conversion to heme by ferrochelatase: one pathway to form heme, which is required for cytochromes, protective roles in non-photosynthetic tissue, and a second for heme and Chl formation in photosynthetic tissue (Singh et al., 2002; Suzuki et al., 2002).

Loss of plastidic ferrochelatase activity by antisense RNA expression in tobacco of the ferrochelatase type II causes accumulation of Proto and, consequently, the formation of necrotic leaf lesions. The activity of a mitochondrial ferrochelatase was not reduced, but could not compensate for lower plastidic ferrochelatase activity. Moreover, excessive Proto attributed for heme synthesis cannot be re-directed to Mg-chelatase suggesting that spatial separation of both ferro- and Mg-chelatase occurs in plastidal sub-compartments as well as tight substrate channeling in multi-enzymatic complexes from the early enzymatic steps through to heme or Chl biosynthesis (Papenbrock et al., 2001).

V. Concluding Remarks

All plant tetrapyrroles are synthesized in plastids with the exception that the last two steps of heme synthesis also occur in mitochondria. All enzymes of the pathway are nuclear-encoded and the genes always encode precursor proteins, which are targeted to their organellar destination. The metabolic flow and the activities of all enzymes are adjusted to developmental, tissue specific, circadian rhythm or environmental conditions. Although each enzymatic step is independently controlled at various steps of gene expression, it is accepted that certain regulatory steps control the general activity of the pathway. Subcellular compartmentation of multi-enzymatic complexes, as well as tight regulation of the expression of each enzyme, is probably essential for appropriate channeling of metabolites between the branched pathways.

In general, tetrapyrrole biosynthesis from ALA to PChlide and protoheme shows some interesting trends: the metabolic intermediates became increasingly hydrophobic and photoreactive. These properties, in turn, affect sub-compartmental location and functions of enzymes involved in photoprotection and substrate channeling. General aspects of enzyme localization, their implication on metabolic flow and the photo-toxic risks of porphyrin accumulation are discussed in Chapter 10, an introductory chapter by Rüdiger and Grimm.

References

Alawady AE and Grimm B (2005) Tobacco Mg protoporphyrin IX methyltransferase is involved in inverse activation of Mg porphyrin and protoheme synthesis. Plant J 41: 282–290

Alawady A, Reski R, Yaronskaya E and Grimm B (2005) Cloning and expression of the tobacco *CHLM* sequence encoding Mg protoporphyrin IX methyltransferase and its interaction with Mg chelatase. Plant Mol Biol 57: 679–691

Arnould S and Camadro JM (1998) The domain structure of protoporphyrinogen oxidase, the molecular target of diphenyl ether-type herbicides. Proc Natl Acad Sci USA 95: 10553–10558

Arnould S, Takahashi M and Camadro JM (1998) Stability of recombinant yeast protoporphyrinogen oxidase: effects of diphenyl ether-type herbicides and diphenyleneiodonium.

Biochemistry 37: 12818–12828
Battersby, AR (1994) How nature builds the pigments of life: the conquest of Vitamin B_{12}. Science 264: 1551–1557
Battersby AR, Fookes CJR, Gustafson-Potter KE, Matcham GWJ and McDonald E (1979a) Proof by synthesis that unrearranged hydroxymethylbilane is the product from deaminase and the substrate for cosynthetase in the biosynthesis of Uro'gen-III. J Chem Soc Chem Commun 1979: 1155–1158
Battersby AR, Fookes CJR, Matcham GWJ and McDonald E (1979b) Order of assembly of the four pyrrole rings during biosynthesis of the natural porphyrins. J Chem Soc Chem Commun 1979: 539–541
Battersby AR, Fookes CJR, Hart G, Matcham GWJ and Pandey PS (1983) Biosynthesis of porphyrins and related macrocycles. Part 21. The interaction of deaminase and its product (hydroxymethylbilane) and the relationship between deaminase and cosynthetase. J Chem Soc Perkin Trans: 3041–3047
Berthold DA and Stenmark P (2003) Membrane-bound diiron carboxylate proteins. Ann Rev Plant Biol 54: 497–517
Birchfield NB, Latli B and Casida JE (1998) Human protoporphyrinogen oxidase: Relation between the herbicide binding site and the flavin cofactor. Biochemistry 37: 6905–6910
Block MA, Tewari AK, Albrieux C, Maréchal E and Joyard J (2002) The plant *S*-adenosyl-*L*-methionine:Mg-protoporphyrin 1X methyltransferase is located in both envelope and thylakoid chloroplast membranes. Eur J Biochem 269: 240–248
Boese QF, Spano AJ, Li J and Timko MP (1991) Aminolevulinic acid dehydratase in pea (*Pisum sarivum* L.). J Biol Chem 266: 17060–17066
Bollivar DW and Beale SI (1995) Formation of the isocyclic ring of chlorophyll by isolated *Chlamydomonas reinhardtii* chloroplasts. Photosynth Res 43: 113–124
Bollivar DW and Beale SI (1996) The chlorophyll biosynthetic enzyme Mg-protoporphyrin IX monomethyl ester (oxidative) cyclase. Plant Physiol 112: 105–114
Bollivar DW, Jiang ZY, Bauer CE and Beale S (1994a) Heterologous expression of the *bchM* gene product from *Rhodobacter capsulatus* and demonstration that it encodes S-adenosyl-*L*-methionine: Mg-protoporphyrin 1X methyltransferase. J Bacteriol 176: 5290–5296
Bollivar DW, Suzuki JY, Beatty JT, Dobrowolski JM and Bauer CE (1994b) Directed mutational analysis of bacteriochlorophyll *a* biosynthesis in *Rhodobacter capsulatus*. J Mol Biol 237: 622–640
Breinig S, Kervinen J, Stith L, Wasson AS, Fairman R, Wlodawer A, Zdanov A and Jaffe EK (2003) Control of tetrapyrrole biosynthesis by alternate quaternary forms of porphobilinogen synthase. Nat Struct Biol 10: 757–763
Castelfranco PA, Weinstein JD, Schwarcz S, Pardo AD and Wezelman BE (1979) The Mg insertion step in chlorophyll biosynthesis. Arch Biochem Biophys 192: 592–598
Che F-S, Watanabe N, Iwano M, Inokuchi H, Takayama S, Yoshida S and Isogai A (2000) Molecular characterization and subcellular localization of protoporphyrinogen oxidase in spinach chloroplasts. Plant Physiol 124: 59–70
Chekounova E, Voronetskaya V, Papenbrock J, Grimm B and Beck CF (2001) Characterization of *Chlamydomonas* mutants defective in the H subunit of Mg-chelatase. Mol Gen Genet 266: 363–373
Chereskin BM, Wong YS and Castelfranco PA (1982) In vitro synthesis of the chlorophyll isocyclic ring. Transformation of Mg-protoporphyrin IX and Mg-protoporphyrin IX monomethyl ester into magnesium-2,4-divinylpheoporphyrin a_5. Plant Physiol 70: 987–993
Cheung KM, Spencer P, Timko MP and Shoolingin-Jordan PM (1997) Characterization of a recombinant pea 5-aminolevulinic acid dehydratase and comparative inhibition studies with the *Escherichia coli* dehydratase. Biochemistry 36: 1148–1156
Choi KW, Han O, Lee HJ, Yun YC, Moon YH, Kim M, Kuk YI, Han SU and Guh JO (1998) Generation of resistance to the diphenyl ether herbicide, oxyfluorfen, via expression of the *Bacillus subtilis* protoporphyrinogen oxidase gene in transgenic tobacco plants. Biosci Biotechnol Biochem 62: 558–560
Chow KS, Singh DP, Walker AR and Smith AG (1998) Two different genes encode ferrochelatase in *Arabidopsis*: Mapping, expression and subcellular targeting of the precursor proteins. Plant J 15: 531–541
Cornah JE, Roper JM, Singh DP and Smith AG (2002) Measurement of ferrochelatase activity using a novel assay suggests that plastids are the major site of haem biosynthesis in both photosynthetic and non-photosynthetic cells of pea (*Pisum sativum* L.). Biochem J 362: 423–432
Crockett N, Alefounder PR, Battersby AR and Abell C (1991) Uroporphyrinogen III synthase: Studies on its mechanism of action molecular biology and biochemistry. Tetrahedron 47: 6003–6014
Dailey HA, Daley TA, Wu CK, Medlock AE, Wang KF, Rose JP and Wang BC (2000) Ferrochelatase at the millennium: Structures, mechanisms and (2Fe-2S) clusters. Cell Mol Life Sci 57: 1909–1926
Duke SO, Becerril JM, Sherman TD, Lehnen LP and Matsumoto H (1991) Protoporphyrinogen oxidase-inhibiting herbicides. Weed Sci 39: 465–473
Ellsworth RK and Dullaghan JP (1972) Activity and properties of *S*-adenosyl-L-methionine: Magnesium-protoporphyrin IX methyltransferase in crude homogenates from wheat seedling. Biochim Biophys Acta 268: 327–333
Ellsworth RK, Dullaghan JP and St. Pierre ME (1974) The reaction mechanism of S-adenosyl-L-methionine: Magnesium protoporphyrin IX methyltransferase of wheat. Photosynth 8: 375–383
Erskine PT, Newbold R, Roper J, Coker A, Warren MJ, Shoolingin-Jordan PM, Wood SP and Cooper JB (1999) The Schiff base complex of yeast 5-aminolaevulinic acid dehydratase with laevulinic acid. Protein Sci 8: 1250–1256
Fodje MN, Hansson A, Hansson M, Olsen JG, Gough S, Willows RD and Al-Karadaghi S (2001) Interplay between an AAA module and an integrin I domain may regulate the function of magnesium chelatase. J Mol Biol 311: 111–122
Frankenberg N, Erskine PT, Cooper JB, Shoolingin-Jordan PM, Jahn D and Heinz DW (1999) High resolution crystal structure of a Mg^{2+}-dependent porphobilinogen synthase. J Mol Biol 289: 591–602
Gibson KD, Neuberger A and Tait GH (1963) Studies on the biosynthesis of porphyrin and bacteriochlorophyll by *Rhodopseudomonas spheriodes*. 4. S-adenosylmethionine-magnesium protoporphyrin methyltransferase. Biochem J 88: 325–334
Gibson LCD and Hunter CN (1994) The bacteriochlorophyll biosynthesis gene, bchM, of *Rhodobacter sphaeroides* encodes *S*-adenosyl-*L*-methionine: Mg protoporphyrin IX methyltransferase. FEBS Lett 352: 127–130
Gibson LCD, Willows RD, Kannangara CG, von Wettstein D

and Hunter CN (1995) Magnesium-protoporphyrin chelatase of *Rhodobacter sphaeroides*: Reconstitution of activity by combining the products of the *bchH, -I*, and *-D* genes expressed in *Escherichia coli*. Biochemistry 92: 1941–1944

Gibson LCD, Marrison JL, Leech RM, Jensen PE, Bassham DC, Gibson M and Hunter CN (1996) A putative Mg chelatase subunit from *Arabidopsis thaliana cv* C24. Plant Physiol 111: 61–71

Goericke R and Repeta DJ (1993) Chlorophylls *a* and *b* and divinyl chlorophylls *a* and *b* in the open subtropical North Atlantic Ocean. Mar Ecol Prog Ser 101: 307–313

Gorchein A (1972) Magnesium protoporphyrin chelatase activity in *Rhodopseudomonas sphaeroides* studies with whole cells. Biochem J 127: 97–106

Gorchein A, Gibson LCD and Hunter CN (1993) Gene expression and control of enzymes for synthesis of magnesium protoporphyrin monomethyl ester in *Rhodobacter sphaeroides*. Biochem Soc Trans 21: 201S

Gough SP, Petersen BO and Duus G (2000) Anaerobic chlorophyll isocyclic ring formation in *Rhodobacter capsulatus* requires a cobalamin cofactor. Proc Natl Acad Sci USA 97: 6908–6913

Grafe S, Saluz HP, Grimm B and Hanel F (1999) Mg-chelatase of tobacco: The role of the subunit CHL D in the chelation step of protoporphyrin IX. Proc Natl Acad Sci USA 96: 1941–1946

Guo R, Luo M and Weinstein JD (1998) Magnesium-chelatase from developing pea leaves. Characterization of a soluble extract from chloroplasts and resolution into three required protein fractions. Plant Physiol 116: 605–615

Hansson A, Kannangara CG, von Wettstein D and Hansson M (1999) Molecular basis for semidominance of missense mutations in the XANTHA-H (42-kDa) subunit of magnesium chelatase. Proc Natl Acad Sci USA 96: 1744–1749

Hansson A, Willows RD, Roberts TH and Hansson M (2002) Three semidominant barley mutants with single amino acid substitutions in the smallest magnesium chelatase subunit form defective AAA^+ hexamers. Proc Natl Acad Sci USA 99: 13944–13949

Hart GJ, and Battersby AR (1985) Purification and properties of uroporphyrinogen III synthase (co-synthase) from *Euglena gracilis*. Biochem J 232: 151–160

Hart GJ, Miller AD and Battersby AR (1987) Evidence that the pyrromethane cofactor of hydroxymethylbilane synthase (porphobilinogen deaminase) is bound through the sulfur atom of a cystein residue. Biochem J 252: 909–912

Higuchi M and Bogorad L (1975) The purification and properties of uroporphyrinogen I synthase and uroporphyrinogen III cosynthase. Interaction between the enzymes. Ann NY Acad Sci 244: 401–418

Hinchigeri SB, Hundle B and Richards WR (1997) Demonstration that the BchH protein of *Rhodobacter capsulatus* activates S-adenosyl-L-methionine:magnesium protoporphyrin IX methyltransferase. FEBS Lett 407: 337–342

Hiriart J-B, Lehto K, Tyystjärvi, Junttila T and Aro E-M (2002) Suppression of a key gene involved in chlorophyll biosynthesis by means of virus-inducing gene silencing. Plant Mol Biol 50: 213–224

Hu G, Yalpani N, Briggs SP and Johal GS (1998) A porphyrin pathway impairment is responsible for the phenotype of a dominant disease lesion mimic mutant of maize. Plant Cell 10: 1095–1105

Hudson A, Carpenter R, Doyle S and Coen ES (1993*) Olive*: A key gene required for chlorophyll biosynthesis in *Antirrhinum majus*. EMBO J 12: 3711–3719

Ishikawa A, Okamoto H, Iwasaki Y and Asahi T (2001) A deficiency of coproporphyrinogen III oxidase causes lesion formation in *Arabidopsis*. Plant J 27: 89–99

Jacobs JM and Jacobs NJ (1987) Oxidation of protoporphyrinogen to protoporphyrin, a step in chlorophyll and haem biosynthesis. Biochem J 244: 219–224

Jacobs JM and Jacobs NJ (1993) Porphyrin accumulation and export by isolated barley (*Hordeum vulgare*) plastids. Plant Physiol 101: 1181–1187

Jensen PE, Gibson LCD, Henningsen KW and Hunter CN (1996a) Expression of the *chlI, chlD,* and *chlH* genes from the cyanobacterium *Synechocystis* PCC6803 in *Escherichia coli* and demonstration that the three cognate proteins are required for magnesium-protoporphyrin chelatase activity. J Biol Chem 271: 16662–16667

Jensen PE, Willows RD, Petersen BL, Vothknecht UC, Stummann BM, Kannangara CG, von Wettstein D and Henningsen KW (1996b) Structural genes for Mg-chelatase subunits in barley: Xantha-*f*, *-g* and *-h*. Mol Gen Genet 250: 383–394

Jensen PE, Gibson LCD and Hunter CN (1999a) ATPase activity associated with the magnesium-protoporphyrin IX chelatase enzyme of *Synechocystis* PCC6803: evidence for ATP hydrolysis during Mg^{2+} insertion, and the MgATP-dependent interaction of the ChlI and ChlD subunits. Biochem J 339: 127–134

Jensen PE, Gibson LCD, Shephard F, Smith V and Hunter CN (1999b) Introduction of a new branchpoint in tetrapyrrole biosynthesis in *Escherichia coli* by co-expression of genes encoding the chlorophyll-specific enzymes magnesium chelatase and magnesium protoporphyrin methyltransferase. FEBS Lett 455: 349–354

Jordan PM (1991) The biosynthesis of 5-aminolevulinic acid and its transformation into uroporphyrinogen III. In: Jordan PM (ed) Biosynthesis of Tetrapyrroles, New Comprehensive Biochemistry, Vol 19, pp 1–86. Elsevier, Amsterdam

Jordan PM and Seehra JS (1979) The biosynthesis of uroporphyrinogen III. Order of assembly of the four porphobilinogen molecules in the formation of the tetrapyrrole ring. FEBS Lett 104: 364–366

Jordan PM and Warren MJ (1987) Evidence for a dipyrromethane cofactor at the catalytic site of *Escherichia coli* porphobilinogen deaminase. FEBS Lett 225: 87–92

Kaczor CM, Smith MW, Sangwan I and O'Brian MR (1994) Plant δ-aminolevulinic acid dehydratase. Plant Physiol 104: 1411–1417

Kjemtrup S, Sampson KS, Peele CG, Hguyen LV, Conkling MA, Thompson WF and Robertson D (1998) Gene silencing from plant DANN carried by a Geminivirus. Plant J 14: 91–100

Koch M, Breithaupt C, Kiefersauer R, Freigang J, Huber R and Messerschmidt A (2004) Crystal structure of protoporphyrinogen IX oxidase: A key enzyme in haem and chlorophyll biosynthesis. EMBO J 23:1720–1728.

Koncz C, Mayerhofer R, Koncz-Kalman Z, Nawrath C, Reiss B, Redei GP and Schell J (1990) Isolation of a gene encoding a novel chloroplast protein by T-DNA tagging in *Arabidopsis thaliana*. EMBO J 9: 1337–1346

Kruse E, Mock HP and Grimm B (1995a) Coproporphyrinogen III oxidase from barley and tobacco — sequence analysis and initial expression studies. Planta 196: 796–803

Kruse E, Mock H-P and Grimm B (1995b) Reduction of copro-

porphyrinogen oxidase level by antisense RNA synthesis leads to deregulated gene expression of plastid proteins and affects the oxidative defense system. EMBO J 14: 3712–3720

Kruse E, Mock HP and Grimm B (1997) Isolation and characterisation of tobacco (*Nicotiana tabacum)* cDNA clones encoding proteins involved in magnesium chelation into protoporphyrin IX. Plant Mol. Biol 35: 1053–1056

Lecerof D, Fodje M, Hansson A, Hansson M and Al-Karadaghi S (2000) Structural and mechanistic basis of porphyrin metallation by ferrochelatase. J Mol Biol 297: 221–232

Lee HJ, Ball MD, Parham R and Rebeiz CA (1992) Chloroplast Biogenesis 65. Enzymic conversion of protoporphyrin IX to Mg-protoporphyrin IX in a subplastidic membrane fraction of cucumber etiochloroplasts. Plant Physiol 99: 1134–1140

Lee HJ, Lee SB, Chung JS, Han SU, Han O, Guh JO, Jeon JS, An G and Back K (2000) Transgenic rice plants expressing a *Bacillus subtilis* protoporphyrinogen oxidase gene are resistant to diphenyl ether herbicide oxyfluorfen. Plant Cell Physiol 41: 743–749

Lermontova I and Grimm B (2000) Overexpression of plastidic protoporphyrinogen IX oxidase leads to resistance to the diphenyl-ether herbicide acifluorfen. Plant Physiol. 122: 75–84

Lermontova I, Kruse E, Mock H-P and Grimm B (1997) Cloning and characterization of a plastidal and a mitochondrial isoform of tobacco protoporphyrinogen 1X oxidase. Proc Natl Acad Sci USA 94: 8895–8900

Li X, Vollrath S, Nicholl DBG, Chilcott CE, Johnson MA, Ward ER and Law MD (2003) Development of protoporphyrinogen oxidase as an efficient selection marker for *Agrobacterium tumefaciens*-mediated transformation of maize. Plant Physiol 133: 736–747

Lim SI, Witty M, Wallace-Cook ADM, Hag LI and Smith AG (1994) Porphobilinogen deaminase is encoded by a single gene in *Arabidopsis thaliana* and is targeted to the chloroplasts. J Mol Biol 26: 863–872

Lister R, Chew O, Rudhe C, Lee M-N and Whelan J (2001) *Arabidopsis thaliana* ferrochelatase-I and -II are not imported into *Arabidopsis* mitochondria. FEBS Lett 506: 291–295

Louie GV, Brownlie PD, Lambert R, Cooper JB, Blundell TL, Wood SP, Malashkevich VN, Hadener A, Warren MJ and Schoolingin-Jordan PM (1996) The three-dimensional structure of *Escherichia coli* porphobilinogen deaminase at 1.76-Å resolution. Proteins 25: 48–78

Luo J and Lim CK (1993) Order of uroporphyrinogen III decarboxylation on incubation of porphobilinogen and uroporphyrinogen III with erythrocyte uroporphyrinogen decarboxylase. Biochem J 289: 529–532.

Luo M, Weinstein JD and Walker CJ (1999) Magnesium chelatase subunit D from pea: Characterization of the cDNA, heterologous expression of an enzymatically active protein and immunoassay of the native protein. Plant Mol Biol 41: 721–731

Martins BM, Grimm B, Mock H-P, Huber R and Messerschmidt A (2001Crystal structure and substrate binding modeling of the uroporphyrinogen-III decarboxylase from *Nicotiana tabacum*. Implications for the catalytic mechanism. J Biol Chem 276: 44108–44116

Masuda T, Suzuki T, Shimada H, Ohta H and Takamiya K (2003) Subcellular localization of two types of ferrochelatase in cucumber. Planta 217: 602–609

Mathews MA, Schubert HL, Whitby FG, Alexander KJ, Schadick K, Bergonia HA, Phillips JD and Hill CP (2001). Crystal structure of human uroporphyrinogen III synthase. EMBO J 20: 5832–5839

Matringe M and Scalla R (1988) Effects of acifluorfen-methyl on cucumber cotyledons: Porphyrin accumulation. Pestic Biochem Physiol 32: 164–172

Matringe M, Camadro JM, Joyard J and Douce R (1994) Localization of ferrochelatase activity within mature pea chloroplasts. J Biol Chem 269: 15010–15015

Matters GL and Beale SI (1995a) Structure and expression of the *Chlamydomonas reinhardtii alad* gene encoding the Chl biosynthetic enzyme, δ-aminolevulinic acid dehydratase (porphobilinogen synthase). Plant Mol Biol 27: 607–617

Matters GL and Beale SI (1995b) Blue-light-regulated expression of genes for two early steps of chlorophyll biosynthesis in *Chlamydomonas reinhardtii*. Plant Physiol 109: 471–479

Miyamoto K, Tanaka R, Teramoto H, Masuda T, Tsuji H and Inokuchi H (1994) Nucleotide sequence of cDNA clones encoding ferrochelatase from barley and cucumber. Plant Physiol 105: 769–770

Mochizuki N, Brusslan JA, Larkin R, Nagatani A and Chory J (2001*) Arabidopsis genomes uncoupled 5 (GUN5)* mutant reveals the involvement of Mg-chelatase H subunit in plastid-to-nucleus signal transduction. Proc Natl Acad. Sci USA 98: 2053–2058

Mock HP and Grimm B (1997) Reduction of uroporphyrinogen decarboxylase by antisense RNA expression affects activities of other enzymes involved in tetrapyrrole biosynthesis and leads to light-dependent necrosis. Plant Physiol 113: 1101–1112

Mock HP, Trainotti L, Kruse E and Grimm B (1995) Isolation, sequencing and expression of cDNA sequences encoding uroporphyrinogen decarboxylase from tobacco and barley. Plant Mol Biol 28: 245–256

Mock HP, Keetman U, Kruse E, Rank B and Grimm B (1998) Defense responses to tetrapyrrole-induced oxidative stress in transgenic plants with reduced uroporphyrinogen decarboxylase or coproporphyrinogen oxidase activity. Plant Physiol 116: 107–116

Mock HP, Heller W, Molina A, Neubohn B, Sandermann H, Jr. and Grimm B (1999) Expression of uroporphyrinogen decarboxylase or coproporphyrinogen oxidase antisense RNA in tobacco induces pathogen defense responses conferring increased resistance to tobacco mosaic virus. J Biol Chem 274: 4231–4238

Molina A, Volrath S, Guyer D, Maleck K, Ryals J and Ward E (1999) Inhibition of protoporphyrinogen oxidase expression in *Arabidopsis* causes a lesion-mimic phenotype that induces systemic acquired resistance. Plant J 17: 667–678

Moseley JL, Allinger T, Herzog S, Hoerth P, Wehinger E, Merchant S and Hippler M (2002) Adaptation to Fe-deficiency requires remodeling of the photosynthetic apparatus. EMBO J 21: 6709–6720

Murphy MJ and Siegel LM (1973) Sirohaem and sirohydrochlorin. The basis for a new type of porphyrin-relatedf prosthetic group common to both assimilatory and dissimilatory sulfite reductases. J Biol Chem 248: 6911–6919

Nagata N, Tanaka R, Satoh S and Tanaka A (2005) Identification of a vinyl reductase gene for chlorophyll synthesis in *Arabidopsis thaliana* and implications for the evolution of *Prochlorococcus* species. Plant Cell 17: 233–240

Nakayama M, Masuda T, Bando T, Yamagata H, Ohta H and Takamiya K-i (1998) Cloning and expression of the soybean

chlH gene encoding a subunit of Mg-chelatase and localization of the Mg^{2+} concentration-dependent ChlH protein within the chloroplast. Plant Cell Physiol 39: 275–284

Nasrulhaq-Boyce A, Griffiths WT and Jones OTG (1987) The use of continuous assays to characterize the oxidative cyclase that synthesizes the chlorophyll isocyclic ring. Biochem J 243: 23–29

Orsat B, Monfort A, Chatellard P and Stutz E (1992) Mapping and sequencing of an actively transcribed *Euglena gracilis* chloroplast gene (*ccsA*) homologous to the *Arabidopsis thaliana* nuclear gene *cs* (*ch42*). FEBS Lett 303: 181–184

Papenbrock J, Gräfe S, Kruse E, Hänel F and Grimm B (1997) Mg-chelatase of tobacco: Identification of a *Chl D* cDNA sequence encoding a third subunit, analysis of the interaction of the three subunits with the yeast two-hybrid system, and reconstitution of the enzyme activity by co-expression of recombinant CHL D, CHL H and CHL I. Plant J 12: 981–990

Papenbrock J, Mock H-P, Kruse E and Grimm B (1999) Expression studies in tetrapyrrole biosynthesis: Inverse maxima of magnesium chelatase and ferrochelatase activity during cyclic photoperiods. Planta 208: 264–273

Papenbrock J, Mock H-P, Tanaka R, Kruse E and Grimm B (2000a) Role of magnesium chelatase activity in the early steps of the tetrapyrrole biosynthetic pathway. Plant Physiol 122: 1161–1169

Papenbrock J, Pfündel E, Mock H-P and Grimm B (2000b) Decreased and increased expression of the subunit CHL I diminishes Mg chelatase activity and reduces chlorophyll synthesis in transgenic tobacco plants. Plant J 22: 155–164

Papenbrock J, Mishra S, Mock H-P, Kruse E, Schmidt E-K, Petersmann A, Braun H-P and Grimm B (2001) Impaired expression of the plastidic ferrochelatase by antisense RNA synthesis leads to a necrotic phenotype of transformed tobacco plants. Plant J 28: 41–50

Parham R and Rebeiz CA (1992) Chloroplast biogenesis: [4-Vinyl] chlorophyllide *a* reductase is a divinyl chlorophyllide *a*-specific, NADPH-dependent enzyme. Biochemistry 31: 8460–8464

Petersen BL, Jensen PE, Gibson LCD, Stummann BM, Hunter CN and Henningsen KW (1998) Reconstitution of an active magnesium chelatase enzyme complex from the *bchl, -D,* and *-H* gene products of the green sulfur bacterium *Chlorobium vibrioforme* expressed in *Escherichia coli*. J Bacteriol 180: 699–704

Petersen BL, Møller MG, Jensen PE and Henningsen KW (1999) Identification of the *Xan-g* gene and expression of the Mg-chelatase encoding genes *Xan-f*, *-g* and *-h* in mutant and wild type barley *(Hordeum vulgare* L*)*. Hereditas 131: 165–170

Pinta V, Picaud M, Reiss-Husson F and Astier C (2002) *Rubrivivax gelantinosus acsF* (previously *orf358*) codes for a conserved, putative binuclear-iron-cluster-containing protein involved in aerobic oxidative cyclization of Mg-protoporphyrin IX monomethylester. J Bacteriol 184: 746–753

Porra RJ and Lascelles J (1968) Studies on ferrochelatase: the enzymic formation of haem in proplastids, chloroplasts and plant mitochondria. Biochem J 108: 343–348

Porra RJ, Barnes R and Jones OTG (1973) The over-production of poprphyrins by semi-anaerobic yeast. Enzyme 16: 1–8

Porra RJ, Schäfer W, Katheder I and Scheer H (1995) The derivation of the oxygen atoms of the 13´-oxo and 3-acetyl groups of bacteriochlorophyll *a* from water in *Rhodobacter sphaeroides* cells adapting from respiratory to photosynthetic conditions: evidence for an anaerobic pathway for the formation of isocyclic ring E. FEBS Lett 371: 21–24

Porra RJ, Urzinger M, Winkler J, Bubenzer C, and Scheer H (1998) Biosynthesis of the 3-acetyl and 13^1-oxo groups of bacteriochlorophyll *a* in the facultative aerobic bacterium, *Rhodovulum sulfidophilum:* The presence of both oxygenase and hydratase pathways for isocyclic ring formation. Eur J Biochem 252: 185–191

Randolph-Anderson BL, Sato R, Johnson AM, Harris EH, Hauser CR, Oeda K, Ishige F, Nishio S, Gillham NW and Boynton JE (1998) Isolation and characterization of a mutant protoporphyrinogen oxidase gene from *Chlamydomonas reinhardtii* conferring resistance to porphyric herbicides. Plant Mol Biol 38: 839–859

Rebeiz CA, Wu SM, Kuhagja M, Daniell H and Perkins EJ (1983) Chlorophyll *a* biosynthetic routes and chlorophyll *a* chemical heterogeneity in plants. Mol Cell Biochem 57: 97–125

Rimington C and Miles PA (1951) A study of porphyrins excreted in the urine by a case of congenital porphyria . Biochem J 50: 202–206

Rissler HM, Collakova E, DellaPenna D, Whelan J and Pogson BJ (2002) Chlorophyll biosynthesis. Expression of a second *Chl I* gene of magnesium chelatase in *Arabidopsis* supports only limited chlorophyll synthesis. Plant Physiol 128: 770–779

Roper JM and Smith AG (1997) Molecular localization of ferrochelatase in higher plant chloroplasts. Eur J Biochem 246: 32–37

Santana MA, Pihakaski-Maunsbach K, Sandal N, Marcker KA and Smith AG (1998) Evidence that the plant host synthesizes the heme moiety of leghemoglobin in root nodules. Plant Physiol 116: 1259–1269

Scalla R, Matringe M, Camadro JM and Labbe P (1990) Recent advances in the mode of action of diphenyl ether and related herbicides. Z Naturforsch 45c: 503–511

Schaumburg A and Schneider-Poetsch HAW (1992) Characterization of plastid 5-aminolevulinate dehydratase (ALAD; EC 4.2.1.24) from spinach (*Spinacia oleracea*) by sequencing and comparison with non-plant ALAD enzymes. Z Naturforsch 47c: 77–84

Schubert HL, Raux E, Matthews MA, Phillips JD, Wilson KS, Hill CP and Warren MJ (2002) Structural diversity in metal ion chelation and the structure of uroporphyrinogen III synthase. Biochem Soc Trans 30: 595–600

Senior NM, Brocklehurst K, Cooper JB, Wood SP, Erskine P, Shoolingin-Jordan PM, Thomas PG and Warren MJ (1996) Comparative studies on the 5-aminolaevulinic acid dehydratases from *Pisum sativum*, *Escherichia coli* and *Saccharomyces cerevisiae*. Biochem J 320: 401–412

Shalygo NV, Averina NG, Grimm B and Mock H-P (1997) Influence of cesium on tetrapyrrole biosynthesis in etiolated and greening barley leaves. Physiol Plant 99: 160–168

Shalygo NV, Mock H-P, Averina NG and Grimm B (1998) Photodynamic action of uroporphyrin and protochlorophyllide in greening barley leaves treated with cesium chloride. J Photochem Photobiol 42: 151–158

Singh DP, Cornah JE, Hadingham S and Smith AG (2002) Expression analysis of the two ferrochelatase genes in *Arabidopsis* in different tissues and under stress conditions reveals their different roles in haem biosynthesis. Plant Mol Biol 50: 773–788

Smith AG (1988) Subcellular localization of two porphyrin-synthesis enzymes in *Pisum sativum* (pea) and *Arum* (cuckoo-pint)

species. Biochem J 249: 423–428

Smith AG, Marsh O and Elder GH (1993) Investigation of the subcellular location of the tetrapyrrole-biosynthesis enzyme coproporphyrinogen oxidase in higher plants. Biochem J 292: 503–508

Smith AG, Santana MA, Wallace-Cook AD, Roper JM and Labbe-Bois R (1994) Isolation of cDNA encoding chloroplast ferrochelatase from *Arabidopsis thaliana* by functional complementation of a yeast mutant. J Biol Chem 259: 13405–13413

Smith CA, Suzuki JY and Bauer CE (1996) Cloning and characterization of the chlorophyll biosynthesis gene *chlM* from *Synechocystis* PCC 6803 by complemention of a bacteriochlorophyll biosynthesis mutant of *Rhodobacter capsulatus.* Plant Mol Biol 30: 1307–1314

Stark WM, Hawker CJ, Hart GJ, Philippides A, Petersen PM, Lewis JD, Leeper FJ and Battersby AR (1993) Biosynthesis of porphyrins and related macrocycles. Part 40. Synthesis of a spiro-lactam related to the proposed spiro-intermediate for porphyrin biosynthesis: Inhibition of cosynthetase. J Chem Soc Perkin Trans I 1993: 2875–2891

Suzuki JY and Bauer CE (1995) Altered monovinyl and divinyl protochlorophyllide pools in *bchJ* mutants of *Rhodobacter capsulatus.* Possible monovinyl substrate discrimination of light-independent protochlorophyllide reductase. J Biol Chem 270: 3732–3740

Suzuki T, Masuda T, Inokuchi H, Shimada H, Ohta H and Takamiya K-i (2000) Overexpression, enzymatic properties and tissue localization of a ferrochelatase of cucumber. Plant Cell Physiol 41: 192–199

Suzuki T, Masuda T, Singh DP, Tan F-C, Tohru T, Shimada H, Ohta H, Smith AG and Takamiya K-i (2002) Two types of ferrochelatase in photosynthetic and non- photosynthetic tissues of cucumber; their difference in phylogeny, gene expression and localization. J Biol Chem 277: 4731–4737

Tripathy BC and Rebeiz CA (1988) Chloroplast biogenesis 60: Conversion of divinyl protochlorophyllide to monovinyl protochlorophyllide in green(ing) barley, a dark monovinyl/light divinyl plant species. Plant Physiol 87: 89–94

Walker CJ and Weinstein JD (1991) In vitro assay of the chlorophyll biosynthetic enzyme Mg-chelatase: Resolution of the activity into soluble and membrane-bound fractions. Biochemistry 88: 5789–5793

Walker CJ and Willows RD (1997) Mechanism and regulation of Mg-chelatase. Biochem J 327: 321–333

Walker CJ, Castelfranco PA and Whyte BJ (1991) Synthesis of divinyl protochlorophyllide. Enzymological properties of the Mg-protoporphyrin 1X monomethyl ester oxidative cyclase system. Biochem J 276: 691–697

Watanabe N, Che F-S, Iwano M, Takayama S, Nakano T, Yoshida S and Isogai A (1998) Molecular characterization of photomixotrophic tobacco cells resistant to protoporphyrinogen oxidase-inhibiting herbicides. Plant Physiol 118: 751–758

Watanabe N, Che F-S, Iwano M, Takayama S, Yoshida S and Isogai A (2001) Dual targeting of spinach protoporphyrinogen oxidase II to mitochondria and chloroplasts by alternative use of two in-frame initiation codons. J Biol Chem 276: 20474–20481

Watanabe N, Takayama S, Yoshida S, Isogal A and Fang-Sik C (2002) Resistance to protoporphyrinogen oxidase-inhibiting compound S23142 from overproduction of mitochondrial protoporphyrinogen oxidase by gene amplification in photomixotrophic tobacco cells. Biosci Biotechnol Biochem 66: 1799–1805

Whitby FG, Phillips JD, Kushner JP and Hill CP (1998) Crystal structure of human uroprophyrinogen decarboxylase. EMBO J 17: 2463–2471

Whyte BJ, Vijayan P and Castelfranco PA (1992) In vitro synthesis of protochlorophyllide: effects of Mg^{2+} and other cations on the reconstituted (oxidative) cyclase. Plant Physiol Biochem 30: 279–284

Willows RD and Beale SI (1998) Heterologous expression of the *Rhodobacter capsulatus bchI, -D*, and *-H* genes that encode magnesium chelatase subunits and characterization of the reconstituted enzyme. J Biol Chem 273: 34206–34213

Willows RD, Gibson LCD, Kanangara CG, Hunter CN and von Wettstein D (1996) Three separate proteins constitute the magnesium chelatase of *Rhodobacter sphaeroides.* Eur J Biochem 235: 438–445

Witty M, Wallace-Cook ADM, Albrecht H, Spano AJ, Michel H, Shabanowitz J, Hunt DF, Timko MP and Smith AG (1993) Structure and expression of chloroplast-localized porphobilinogen deaminase from pea (*Pisum sativum* L.) isolated by redundant polymerase chain reaction. Plant Physiol 103: 139–147

Wong Y-S and Castelfranco PA (1984) Properties of the Mg-protoporphyrin IX monomethyl ester (oxidative) cyclase system. Plant Physiol 79: 730–733

Wong Y-S, Castelfranco PA, Goff DA and Smith KM (1985) Intermediates in the formation of the chlorophyll isocyclic ring. Plant Physiol 79: 725–729

Wu CK, Dailey HA, Rose JP, Burden A, Sellers VM and Wang BC (2001) The 2.0 A structure of human ferrochelatase, the terminal enzyme of heme biosynthesis. Nat Struct Biol 8: 156–160

Zheng CC, Porat R, Lu P and O'Neill SD (1998) PNZIP is a novel mesophyll-specific cDNA that is regulated by phytochrome and the circadian rhythm and encodes a protein with a leucine zipper motif. Plant Physiol 116: 27–35